BJPS

Brazilian Journal of
Pharmaceutical Sciences

http://dx.doi.org/10.1590/s2175-97902023e22430

Article

Electrochemical immunosensing of low-density lipoprotein based on sol-gel encapsulation

Elton Max Nascimento do Egito[1,2], Isaac Aaron Morales Frias[1,2], Maria Danielly Lima Oliveira[1,2], César Augusto Souza de Andrade[1,2*]

[1]Programa de Pós-Graduação em Inovação Terapêutica, Centro de Biociências, Universidade Federal de Pernambuco, Recife, PE, Brasil, [2]Laboratório de Biodispositivos Nanoestruturados, Universidade Federal de Pernambuco, Recife, PE, Brasil

Lipoprotein monitoring is desirable in the management of medical conditions such as atherosclerotic cardiovascular disease and coronary artery disease, in which controlling the concentration of these chylomicrons is crucial. Current clinical methods are complex and present poor reproducibility between laboratories. For these reasons, recent guidelines discard the assessment of low-density lipoprotein cholesterol (LDL-C) as a routine analysis during lipid-lowering therapies. Concerning the importance of monitoring this parameter, the authors present an electrochemical immunosensor constructed from a simple and easy-to-reproduce platform that allows detecting and quantifying LDL nanoparticles directly from human serum samples. The performance of the biosensor was studied by scanning electron microscopy, cyclic voltammetry, and electrochemical impedance spectroscopy. The biosensing platform displays good stability and linearity between 30 mg dL^{-1} and 135 mg dL^{-1} with a detection limit of 20 mg dL^{-1}. The proposed biosensor can be easily employed for monitoring LDL concentration in clinical treatments.

Keywords: Apolipoprotein. Biosensor. Electrochemistry. Hypercholesterolemia. Self-assembled monolayer. Sol-gel.

INTRODUCTION

Several studies have demonstrated the relationship between high levels of low-density lipoprotein (LDL) nanoparticles and the risk of cardiovascular disease (CVD) of coronary artery disease (CAD) (Williams *et al*., 2014). Also, guidelines have promoted a broader approach to lipid-associated risk assessment (Packard, 2022). Besides its clinical importance, cholesterol is an essential molecule required for the metabolism of fats, hormones, and vitamin D (Bogh *et al.,* 2010). The fast and accurate monitoring of LDL concentration assesses the impact of aggressive lipid-lowering on CAD progression (Libby, 2015). In most clinical laboratories LDL concentration is usually determined by quantification methods such as chemical precipitation, immunoseparation (Nauck, Warnick, Rifai, 2002), or indirectly, by the Friedewald equation (Teoh, Weerasinghe, 2015). The complexity of these methodologies evidences their impracticability during continuous monitoring. In 2015, the American College of Cardiology/American Heart Association (ACC/AHA) removed the low-density lipoprotein cholesterol (LDL-C) assessment as a performance measure to monitor the development of atherosclerotic cardiovascular disease. The 2019 dyslipidemia guidelines from the European Society of Cardiology universally classify patients with LDL-C levels of greater than 190 mg/dL as high-risk individuals, with an LDL-C treatment goal of less than 70 mg/dL (Mortensen *et al.,* 2022).

Compared to the extensive time and supplies consumed during conventional monitoring, biosensors are a profitable quick tool that, being pre-prepared, is ready to be used even by inexperienced users.

***Correspondence:** C. A.S. Andrade. Laboratório de Biodispositivos Nanoestruturados. Departamento de Bioquímica. Universidade Federal de Pernambuco. 50670-901, Recife, PE, Brazil. Phone: +55 81 2126.8450; Fax: +55 81 2126.8547. E-mail: csrandrade@gmail.com. ORCID: https://orcid.org/0000-0002-3271-2817

Biosensors are specific, sensitive, and easy to use, although their manufacturing protocols are not always straightforward. The ionic strength of the electrolyte solution, pH, temperature, convenient amine-free buffer, and degasification are some of the critical factors that must be controlled during the fabrication of biosensors envisaged under covalent immobilization protocols (Fischer, 2010). Addressing these challenges, the research community has been creating a new generation of POC biosensors inspired by recent advances in chemistry, material sciences, and device engineering (Cheon *et al.,* 2022). For these reasons, the development of more straightforward strategies to achieve a stable platform is desirable.

The application of electrochemical biosensors on LDL quantification does not require extreme detection limits. The clinical interest of LDL levels in humans varies from 40 mg dL^{-1} to 190 mg dL^{-1} (Berry-Kravis *et al.,* 2015). Because of the required range of detection, fast and economical solutions can be favored to construct reproducible and sensible biosensors. Platforms developed from self-assembled monolayers (SAMs) are simple systems that allow tailoring of the interfacial properties of metal, metal oxide, and semiconductor surfaces (Costa *et al.,* 2014). In this context, polymeric SAMs as electrochemical platforms require minimal preparation and handling.

Synthetic polymers such as polyacrylamide, polyvinyl alcohol, polyvinyl chloride, and polyvinyl formal (PVF), seize intrinsic properties such as flexibility, higher mechanical strength, and chemical resistance (Khun *et al.*, 2012). Thus, SAMs fabricated from these materials form an extremely strong molecule–substrate interaction through molecular assembly, whereby chemical bonds are formed at the interface (Kim, Yoo, 2021). In addition, their final porosity allows final structures with mechanical and thermal stability that can be used to encapsulate materials within the mean size of their pores (Jerónimo *et al.,* 2007). Many functional groups have demonstrated affinity toward the metallic surface of gold nanoparticles such as COO-, SH, and hydrophobically modified polycations (Remant Bahadur *et al.,* 2006; Park, Shumaker-Parry, 2014). In the case of PVF, the affinity of gold nanoparticles with PVF can be explained in terms of hydrophobic interactions. Furthermore, earlier reports describe the stable interaction between polyvinyl formal SAM and a gold surface for electrochemical applications (Oliveira *et al.,* 2011). The bioreceptor layer is the critical element of biosensor design (Wasilewski *et al.,* 2022). This work presents an electrochemical approach based on the peculiar characteristic of PVF to form self-organized microporous films. Gold nanoparticles (AuNPs) were implemented to avail their high surface-to-volume ratio, and strong adsorption ability to immobilize specific antibodies for apolipoprotein B-100 found on the surface of every LDL nanoparticle. In this manner, we developed a self-assembled PVF film employed as porous support to encapsulate antibody/gold-nanoparticle biorecognition complexes. This simplicity allowed us to evaluate the concentration of LDL directly from human serum without requiring a label or reporter molecule.

MATERIAL AND METHODS

Material

Polyvinyl formal (PVF), Gold(III) chloride trihydrate, sodium citrate, ferro, and ferri cyanide ($K_4[Fe(CN)_6]/K_3[Fe(CN)_6]$) were purchased from Sigma-Aldrich (St. Louis, USA). Chloroform, sodium phosphate monobasic, and sodium phosphate dibasic were obtained from Dinâmica, São Paulo Brazil. Mouse / IgG1Apolipoprotein B Monoclonal Antibody was purchased from Thermo Fischer (USA, F2C9). Deionized (DI) water was obtained from a Milli-Q water purification system (Billerica, MA, USA).

Synthesis of Gold/PVF System.

Colloidal gold was prepared according to the Frens method (Zhang *et al.,* 2014). An absorbance band of the citrate-capped AuNPs solution was recorded at 527nm to confirm nanoparticle synthesis. The solution was stored at 4°C in a dark-colored glass bottle until use. 1 mL of a 0.1% PVF chloroform solution was mixed with 150µL of the AuNPs solution and vortex-mixed vigorously for 2 minutes to obtain the PVF-AuNPs system.

Electrochemical Measurements

Electrochemical measurements were performed using a PGSTAT 128N potentiostat interfaced with NOVA 1.8 software. Throughout the investigation, a three-electrode setup with an Ag/AgCl (saturated in KCl), reference electrode, and working electrode was employed. A platinum wire and a modified gold disc (= 2mm) were used as auxiliary and working electrodes.

Cyclic voltammetry (CV) was performed by sweeping a potential from -0.2V to +0.7 at a scan rate of 50 $mV.s^{-1}$. Electrochemical impedance spectroscopy (EIS) measurements were recorded in a frequency range from 100 mHz to 100 kHz. The amplitude of the applied sine wave potential was 10 mV. The direct current (dc) potential was limited at the open circuit potential measured just before its application. CV and EIS measurements were performed in the presence of a 10mM $K_4[Fe(CN)_6]/K_3[Fe(CN)_6]$ (1:1) redox probe solution in buffer (PBS) at pH 7.4 and carried out during different construction stages of the electrode. All electrochemical measurements were performed at room temperature and inside a Faraday cage.

Construction of the biosensor and measuring LDL samples

Human blood samples (n = 3) were obtained through peripheral venipuncture (without anticoagulants) in the Clinical Laboratory Gilson Cidrim LTDA (Recife, Brazil). The samples were centrifuged at 3000 rpm for 15 min to obtain human serum. The concentration of LDL present in sera samples was validated beforehand by the colorimetric method measuring enzymatic byproducts of LDL oxidation using an ADVIA 1800 Chemistry System. The gold electrode was initially cleaned using thin 1200-mesh sandpaper, then polished with alumina slurry 0.04 μm, and finally washed in an ultrasonic bath in ultrapure water for 5 min and dried. Before adopting a protocol to construct our platform, we explored the conditions to achieve the optimal time of incubation required to coat the bare gold electrode with the encapsulating matrix. We aimed to enhance the stability and electrical response caused by the PVF-AuNPs self-assembled film atop the gold electrode surface. We monitored the decrease in conductivity of the anodic potential peak vs incubation time. We found that after 20 min of incubation EPa was stable around 23 μA being enough to cover the surface of the gold electrode. Following this, we proceeded to study the electrical response after the adsorption of monoclonal antibody (MAb). After constructing the modified electrode system with the encapsulating matrix, 1 μL of MAb solution was added dropwise, allowing 1 min incubation time at room temperature. Passed this time, in the same manner, we added 1 μL of a 10% BSA solution in PBS at pH 7.4. The platform was incubated for 5 minutes to block all non-specific binding sites that remained free after MAb adsorption (Costa *et al.,* 2017). Once the electrical signal was stable, we evaluated 1 μL of the human serum samples containing different LDL concentrations (30, 70, 95, 115, and 135 mg dL^{-1}). Each analysis, performed by CV and EIS, was repeated three separate times and performed under the same technical conditions.

RESULTS AND DISCUSSION

Morphological Analysis

Morphology was investigated by using a JEOL scanning electron microscopy JSM 5900. Figure 1 shows a schematic representation of the PVF-AuNPs-MAb system and its subsequent interaction with LDL nanoparticles. In Figure 2, we present SEM micrographs captured during different construction stages of the PVF-AuNPs-MAb-BSA modified electrode and after interaction with human LDL nanoparticles present in serum samples. Initially (Figure 2a), the PVF-AuNPs-modified electrode presents a homogeneous distribution of small agglomerates of the encapsulating matrix After incorporating the MAbs solution (Figure 2b), the PVF-AuNPs-MAb-BSA modified electrode increases the number and diameter of the agglomerated masses. As an insert in Figure 2b, we show a magnification of the new aggregates, confirming the change in morphology occurring mainly from the BSA blocking non-passivated sites. In Figure 2c, after testing an LDL-concentrated sample, we notice a fully populated electrode surface. The significant amount of covered surface reveals the successful biomolecular

recognition of LDL based on antibody-antigen-binding interactions. These results confirm that the obtained electrical responses are associated with the biointeraction between the LDL present in the serum samples and the PVF-AuNPs-MAb-BSA modified electrode surface after testing the LDL samples.

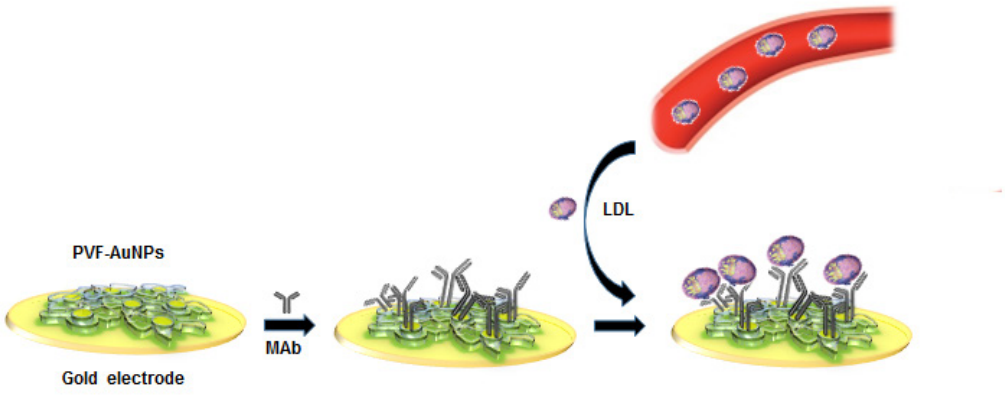

FIGURE 1 - Schematic representation of the encapsulating system interaction with LDL cholesterol molecules.

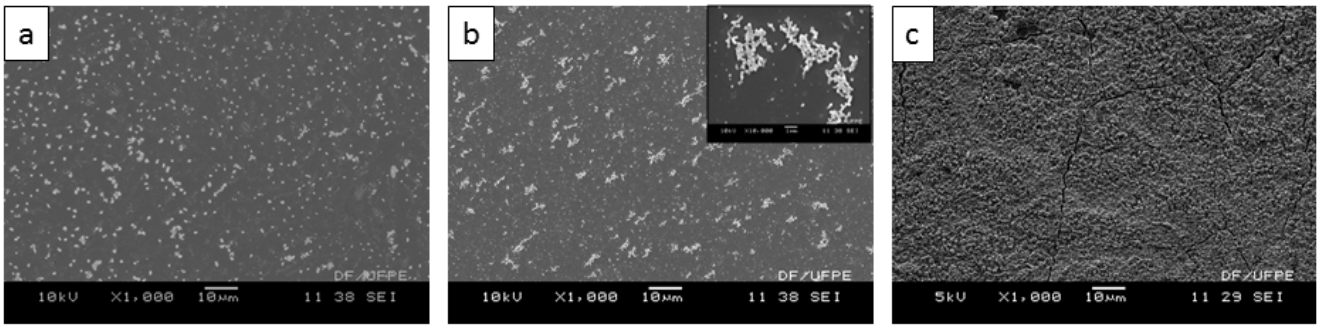

FIGURE 2 - Scanning electron microscopy of the system a) PVF-AuNPs, b) PVF-AuNPs-MAb-BSA, and c) PVF-AuNPS-MAb-BSA-Serum Sample. Inset: magnification of the PVF-AuNPs-MAb-BSA system.

Electrochemical characterization

In Figure 3 we show the EIS and CV characterizations during the different fabrication steps of the biosensor. Electrochemical measurement results are presented in Figure 4. Although serum samples used in this part of the study were previously analyzed to assess LDL concentration, we managed to perform a blind analysis by selecting the samples randomly to be tested. The CV analyses (Figure 3a) provided crucial qualitative information about the nature of the occurring interactions and the number of adsorbed molecules on the electrode surface. Of note, it was observed a gradual decrease in the value of the anodic peak (*ip)* during the fabrication of the PVF-AuNPs-MAb-BSA platform. The analyses performed with patient samples revealed a further reduction in the *ip* values with increasing LDL concentration. This behavior confirms that anti-LDL MAb retained its bioactivity after being adsorbed over the surface of the PVF-AuNPs-MAb-BSA sensor system. The black curve (with the highest *ip*) is the electrochemical response from the redox probe $K_4[Fe(CN)_6]/K_3[Fe(CN)_6]$ of the bare gold electrode. We notice that after the self-assembly of PVF-AuNPs film and after MAb immobilization, the ip decreases, and the potential separation increases between the anodic and cathodic peaks. For the most probable,

the encapsulation of the MAb is sufficient to perturb the redox probe transfer rate at the electrode interface. When the electrode was tested with serum samples, we noticed that concentrations of LDL as low as 30 mg dL^{-1} resulted in a dramatic decrease in the peak current. This behavior demonstrates a continuous interaction between the antibody and its antigen. Furthermore, serum samples containing higher concentrations cause the once different anodic and cathodic current peaks to disappear because of the strong interaction.

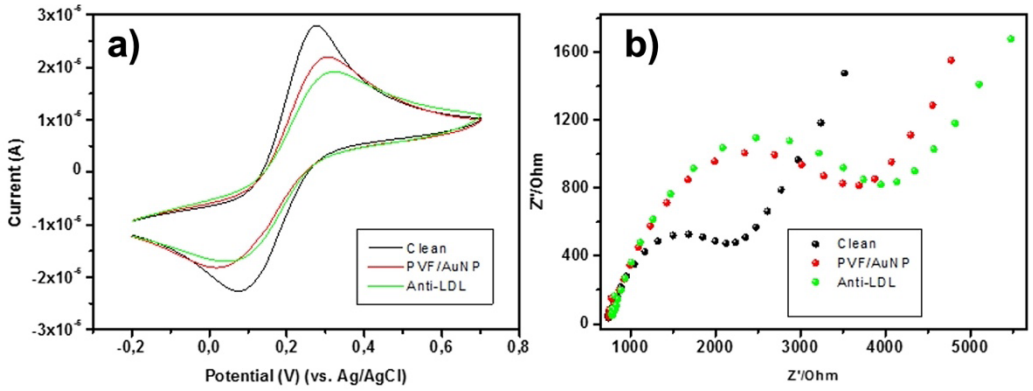

FIGURE 3 - Cyclic voltammograms (a) and electrochemical impedance spectroscopy (b) of the different fabrication steps.

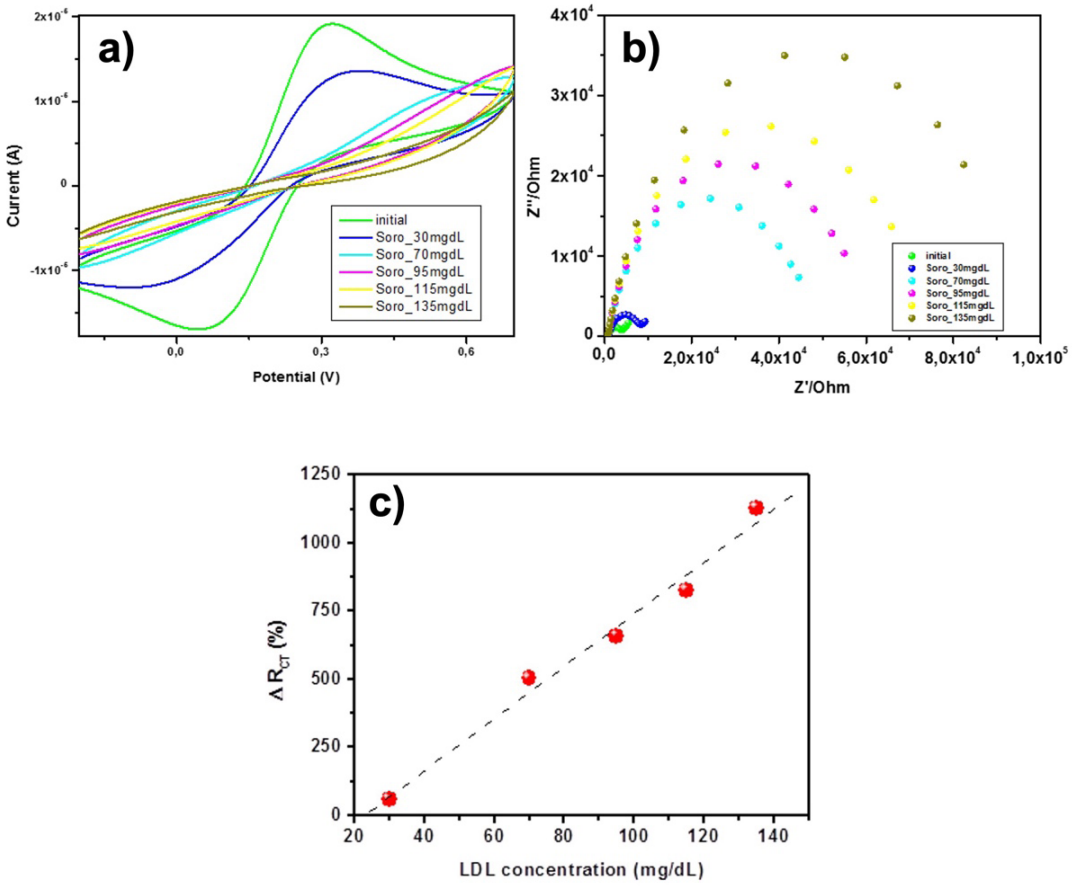

FIGURE 4 - Cyclic voltammograms (a) and electrochemical impedance spectroscopy (b) of the immunosensor exposed the different serum samples (ranging from 30 mg dL^{-1} to 135 mg dL^{-1}). Interpolation between the serum concentration and ΔR_{CT} (c).

Impedance spectra of the sensor system were systematically evaluated during the fabrication process (Figure 3b). The impedimetric responses were analyzed employing a modified Randle's equivalent circuit calculated using NOVA 1.8 software. The studied circuit includes (i) Rs, the ohmic resistance of the electrolyte solution; (ii) W, the Warburg impedance caused by the diffusion of ions from the bulk electrolyte to the electrode interface; (iii) a double layer capacitance (Cpl); and (iv) Rct related to the charge transfer resistance occurring on the surface of the electrode. The resultant fitting is shown as black lines jointly with experimental scattered points. The diameters of the impedimetric semicircle increase proportionally to the LDL concentration in each serum sample. The equivalent circuit results show that this incremental behavior is related to the amount of charge transfer resistance (Rct). This response is most probably caused because negative charges carried by the LDL molecules blocking the electron transfer of the redox probe. Therefore, the increasing response of the resistive component is derived from the biorecognition event occurring between the MAb and its antigen B100 apolipoprotein. The hampered flow of the redox probe to the gold electrode suggests the presence of a self-assembled LDL layer.

After the characterization of each equivalent circuit, Rct and Cdl are the electrical parameters that better reflect the variation of the impedance response arising from the antibody-antigen interactions. In this case, the capacitance presents a high impedance as the frequency drops. Thus, Rct was preferred for its direct correlation with the electron transfer rate. Initially, the bare gold electrode presented an Rct of 1.49 kΩ. After the self-assembly of PVF-AuNPs layer, Rct doubled to 3.00 kΩ. Then, when the monoclonal antibody is encapsulated, Rct remained very close to the same value (3.27 kΩ). Obtaining small Rct increments is coherent with the Mab size being around 10 nm in height and 2.5 nm wide (Kamogawa *et al.,* 2012). Consequently, they are adsorbed to the gold nanoparticles encapsulated in the PVF porous film and do not imply a considerable obstruction to the redox probe. Subsequently, we used bovine serum albumin (BSA) to block non-passivated binding sites that could have remained over the surface of the sensing platform. After the adsorption of BSA, we noticed an increase in Rct, reaching a value of 7.68 kΩ. After this point, we consider that the sensor is ready to diagnose the serum samples.

Biorecognition characterization

The biorecognition of LDL apolipoprotein promotes the formation of insulating layers above the sensing platform. Hence, depending on the LDL concentration present in the serum sample, a gradual variation in Rct will occur. The relative variation of the Rct (%ΔRct) is helpful to evaluate the performance of the biosensor and is calculated according to

$$\%\Delta Rct = \left| \frac{Rct_{(PVF-AuNPs-MAb-BSA-LDL)} - Rct_{(PVF-AuNPs-MAb-BSA)}}{Rct_{(PVF-AuNPs-MAb-BSA)}} \right| x\ 100,$$

where $Rct_{(PVF\text{-}AuNPs\text{-}MAb\text{-}BSA\text{-}LDL)}$ is the R_{CT} value after apolipoprotein has bound to MAb, and $Rct_{(PVF\text{-}AuNPs\text{-}MAb\text{-}BSA)}$ is the initial R_{CT} value of PVF-AuNPs-MAb-BSA platform. In Figure 3c, we present a plot of the calculated %ΔRct values versus the LDL concentrations obtained through the standard immunocolorimetric technique. The linearity of the impedimetric response was found from the 30 to 135 mg dL^{-1} range with a coefficient of determination (r^2) of 97.9%. The limit of detection (LOD) was calculated as 20 mg dL^{-1} from the linear regression as 3.3σ/S where σ is the standard deviation of the intercept of the regression line and S is the slope of the calibration curve. The observed correlation results from the successful biorecognition of the MAb towards LDL. Because of this affinity, the progressive mass increase at the surface of the electrode blocks the interface of the gold electrode surface proportionately. The linearity and detection limit attained with this robust and straightforward platform are well-positioned compared to previous works. Table I shows our results and those of other reported LDL immunosensors (Esteban-Fernández de Ávila *et al.,* 2014). Some recent works emphasize the detection of LDL at very low detection limits in the range of ng/mL, but the synthetic samples are pure LDL fabricated in PBS (Rudewicz-Kowalczyk, 2021; Assaifan *et al.,*

2022) and therefore, their applicability in clinal samples is yet to be proven. We highlight that the here presented sol-gel platform can be fabricated in minutes, compared to the hours needed for the covalent immobilization strategies, with the upper hand of avoiding critical steps that may compromise the bioactivity of the antibody. Furthermore, its applicability comes in handy for clinical diagnostics because its detection range falls within the clinical parameters needed by physicians to perform treatment decisions. The device was tested with real human sera samples and validated through a standardized colorimetric methodology well-known in the clinical environment. Finally, we aimed to enhance the stability and electrical response caused by the PVF-AuNPs self-assembled film atop the gold electrode surface (Results shown in Supplementary Material, Table SI).

TABLE I - Comparison of our results and those of other reported LDL immunosensors

Technique	Substrate	Immobilization	Detection limit (mg dL-1)	Preparation Time	Ref.
QCM	Gold Crystal	Covalent EDC-NHS	84	□12h	(Matharu *et al.,* 2009)
Amperometry	SCP Carbon electrode	Covalent EDC-NHS	0.08	□6h	(Esteban-Fernández de Ávila *et al.,* 2014)
EIS	Graphene Oxide	Covalent EDC-NHS	5	□6h	(Ali *et al.,* 2014a)
CV and EIS	Gold coated glass/ Quantum dots	Thioglycolic acid EDC-NHS	16	□36h	(Ali *et al*., 2014b)
CV and EIS	Gold electrode	Thiol-Gold	$0.31x10^{-7}$	□34h	(Rudewicz-Kowalczyk, 2021)
EIS and capacitance	Gold electrode	Thiol-Gold	$7x10^{-5}$	□4h	(Assaifan *et al.,* 2022)
This Work	Gold electrode	Self-assembly	20	10 min	This work

TABLE SI - Conditions to achieve the optimal time of incubation required to coat the bare gold electrode with the encapsulating matrix. Incubation time vs. anodic potential peak (EPa)

Time (min)	5	10	20	30	40	60
EPa (μA)	29	27	23	24	24	24

CONCLUSIONS

The construction of the PVF-AuNPs platform showed to be robust. Our results demonstrate that the PVF-AuNPs system efficiently adsorbed MAbs while the pores of the polymer served as encapsulating matrix preventing their breakout. We found that the biorecognition ability of the MAbs is maintained after their immobilization. The LDL limit of detection calculated from human serum samples was 20 mg $dL^{-1,}$ while the most concentrated analyzed sample was 135 mg dL^{-1}. The biosensing system is appropriate for monitoring applications within the physiological range of LDL concentration in human blood. The fabrication protocol of this platform is simpler, faster, and easier to reproduce when compared to other biosensors or conventional

studies such as immunocolorimetric calculations and ELISA. The proposed system offers several advantages for LDL quantification, for example, small-volume sampling and adaptation for clinical analysis directly from serum samples. Thus, we propose that these biosensors could be used as an alternative for developing fast and cheap point-of-care diagnostic devices.

ACKNOWLEDGMENTS

The authors are grateful for financial support from CNPq and INCT_IF (Instituto Nacional de Ciência e Tecnologia para Inovação Farmacêutica). E.M.N. do Egito would like to Laboratory Gilson Cidrim LTDA for kind cooperation. Isaac A. M. Frías would like to thank CAPES and FACEPE for the postdoctoral fellowship (APQ-0437-4.03/17).

REFERENCES

Ali MA, Kamil Reza K, Srivastava S, Agrawal VV, John R, Malhotra BD. Lipid–lipid interactions in aminated reduced graphene oxide interface for biosensing application. Langmuir. 2014a;30(14):4192–201.

Ali MA, Srivastava S, Pandey MK, Agrawal VV, John R, Malhotra BD. Protein–conjugated quantum dots interface: binding kinetics and label-free lipid detection. Anal Chem. 2014b; 86(3):1710-1718.

Assaifan AK, Alqahtani FA, Alnamlah S, Almutairi R, Alkhammash HI. Detection and Real-Time Monitoring of LDL-Cholesterol by Redox-Free Impedimetric Biosensors. Biochip J [Internet]. 2022;16(2):197–206.

Berry-Kravis E, Levin R, Shah H, Mathur S, Darnell JC, Ouyang B. Cholesterol levels in fragile X syndrome. Am J Med Genet A. 2015;167(2):379–84.

Bogh MKB, Schmedes A v, Philipsen PA, Thieden E, Wulf HC. Vitamin D production after UVB exposure depends on baseline vitamin D and total cholesterol but not on skin pigmentation. J Invest Dermatol. 2010;130(2):546–53.

Cheon J, Qin J, Lee LP, Lee H. Advances in biosensor technologies for infection diagnostics. Acc Chem Res. 2022;55(2):121–2.

Costa MP, Andrade CAS, Montenegro RA, Melo FL, Oliveira MDL. Self-assembled monolayers of mercaptobenzoic acid and magnetite nanoparticles as an efficient support for development of tuberculosis genosensor. J Colloid Interface Sci. 2014;433:141–8.

Costa MP, Frías IAM, Andrade CAS, Oliveira MDL. Impedimetric immunoassay for aflatoxin B1 using a cysteine modified gold electrode with covalently immobilized carbon nanotubes. Microchimica Acta [Internet]. 2017;184(9):3205–13.

Esteban-Fernández de Ávila B, Campuzano S, Pedrero M, Salvador JP, Marco MP, Pingarrón JM. Lipoprotein (a) determination in human serum using a nitrilotriacetic acid derivative immunosensing scaffold on disposable electrodes. Anal Bioanal Chem. 2014;406(22):5379–87.

Fischer MJE. Amine coupling through EDC/NHS: a practical approach. Em: Surface plasmon resonance. Springer; 2010. p. 55–73.

Jerónimo PCA, Araújo AN, Conceição BSM Montenegro M. Optical sensors and biosensors based on sol–gel films. Talanta [Internet]. 2007;72(1):13–27.

Kamogawa M, Shimanuki J, Azuma T, Murakami A, Ishiguro T. Transmission Electron Microscopy Observation of Antibody. Procedia Eng. 2012;36:150–3.

Khun K, Ibupoto ZH, Nur O, Willander M. Development of galactose biosensor based on functionalized ZnO nanorods with galactose oxidase. J Sens. 2012;2012.

Kim S, Yoo H. Self-assembled monolayers: Versatile uses in electronic devices from gate dielectrics, dopants, and biosensing linkers. Micromachines (Basel). 2021;12(5):565.

Libby P. How does lipid lowering prevent coronary events? New insights from human imaging trials. Vol. 36, European heart journal. Oxford University Press; 2015. p. 472–4.

Matharu Z, Bandodkar AJ, Sumana G, Solanki PR, Ekanayake EMIM, Kaneto K, et al. Low density lipoprotein detection based on antibody immobilized self-assembled monolayer: investigations of kinetic and thermodynamic properties. J Phys Chem B. 2009;113(43):14405–12.

Mortensen MB, Caínzos-Achirica M, Steffensen FH, Bøtker HE, Jensen JM, Sand NPR, et al. Association of coronary plaque with low-density lipoprotein cholesterol levels and rates of cardiovascular disease events among symptomatic adults. JAMA Netw Open. 2022;5(2):e2148139–e2148139.

Nauck M, Warnick GR, Rifai N. Methods for measurement of LDL-cholesterol: a critical assessment of direct measurement by homogeneous assays versus calculation. Clin Chem. 2002;48(2):236–54.

Oliveira MDL, Abdalla DSP, Guilherme DF, Faulin TES, Andrade CAS. Impedimetric immunosensor for electronegative low density lipoprotein (LDL−) based on monoclonal antibody adsorbed on (polyvinyl formal)–

gold nanoparticles matrix. Sens Actuators B Chem. 2011;155(2):775–81.

Packard CJ. Remnants, LDL, and the Quantification of Lipoprotein-Associated Risk in Atherosclerotic Cardiovascular Disease. Curr Atheroscler Rep. 2022;1–10.

Park JW, Shumaker-Parry JS. Structural Study of Citrate Layers on Gold Nanoparticles: Role of Intermolecular Interactions in Stabilizing Nanoparticles. J Am Chem Soc. [Internet]. 2014;136(5):1907–21.

Remant Bahadur KC, Aryal S, Bhattarai SR, Bhattarai N, Kim CH, Kim HY. Stabilization of gold nanoparticles by hydrophobically-modified polycations. J Biomater Sci Polym Ed [Internet]. 2006;17(5):579–89.

Rudewicz-Kowalczyk IwonaTI - Detection of Low Density Lipoprotein-Comparison of Electrochemical Immuno- and Aptasensor DG. No Title. Vol. 21, Sensors. 2021.

Teoh Y, Weerasinghe D. Performance of non-HDL cholesterol (via de Cordova equation) and LDL calculated with Friedewald equation compared to LDL cholesterol measured by ultracentrifugation in a lipid clinic population. Atherosclerosis. 2015;241(1):e125.

Wasilewski T, Neubauer D, Kamysz W, Gębicki J. Recent progress in the development of peptide-based gas biosensors for environmental monitoring. Case Stud Chem Environ Eng. 2022;5:100197.

Williams PT, Zhao XQ, Marcovina SM, Otvos JD, Brown BG, Krauss RM. Comparison of four methods of analysis of lipoprotein particle subfractions for their association with angiographic progression of coronary artery disease. Atherosclerosis. 2014;233(2):713–20.

Zhang P, Xi C, Feng C, Xia H, Wang D, Tao X. Transition metal ion-assisted synthesis of monodisperse, quasi-spherical gold nanocrystals via citrate reduction. CrystEngComm. 2014;16(24):5268–74.

Received for publication on 28th July 2022
Accepted for publication on 07th November 2022